Seasonal changes in carbohydrates and water content predict dynamics of frost hardiness in various temperate tree species

Romain Baffoin, Guillaume Charrier, Anne-Emilie Bouchardon, Marc Bonhomme, Thierry Ameglio, André Lacointe

Tree Physiology 41, 1583–1600
https://doi.org/10.1093/treephys/tpab033

Research paper

Seasonal changes in carbohydrates and water content predict dynamics of frost hardiness in various temperate tree species

Romain Baffoin[1], Guillaume Charrier[1,2], Anne-Emilie Bouchardon[1], Marc Bonhomme[1], Thierry Améglio[1] and André Lacointe[1]

[1]Université Clermont Auvergne, INRAE, PIAF, Clermont-Ferrand 63000, France; [2]Corresponding author (guillaume.charrier@inrae.fr)

Received April 22, 2020; accepted February 16, 2021; handling Editor Dr Marilyn Ball

Predicting tree frost tolerance is critical to select adapted species according to both the current and predicted future climate. The relative change in water to carbohydrate ratio is a relevant trait to predict frost acclimation in branches from many tree species. The objective of this study is to demonstrate the interspecific genericity of this approach across nine tree species. In the studied angiosperm species, frost hardiness dynamics were best correlated to a decrease in water content at the early stage of acclimation (summer and early autumn). Subsequently, frost hardiness dynamics were more tightly correlated to soluble carbohydrate contents until spring growth resumption. Based on different model formalisms, we predicted frost hardiness at different clade levels (angiosperms, family, genus and species) with high to moderate accuracy (1.5–6.0 °C root mean squared error (RMSE)) and robustness (2.8–6.1 °C prediction RMSE). The TOT model, taking all soluble carbohydrate and polyols into account, was more effective and adapted for large scale studies aiming to explore frost hardiness across a wide range of species. The ISC model taking the individual contribution of each soluble carbohydrate molecule into account was more efficient at finer scale such as family or species. The ISC model performance also suggests that the role of solutes cannot be reduced to a 'bulk' osmotic effect as could be computed if all of them were located in a single, common, compartment. This study provides sets of parameters to predict frost hardiness in a wide range of species, and clues for targeting specific carbohydrate molecules to improve frost hardiness.

Keywords: frost acclimation, modeling, perennial plants, soluble carbohydrates, starch, water content.

Introduction

In frost-exposed areas (i.e., alpine, boreal and temperate biomes), perennial plants have to transiently increase their frost hardiness (FH) to tolerate potentially damageable freezing temperatures. This process, called frost acclimation, is induced by seasonal changes in meteorological conditions (Christersson 1978). In autumn, frost acclimation is induced by the decreasing photoperiod and cold, but non-freezing, temperatures (Arora and Rowland 2011, Pagter et al. 2011). In late winter, frost deacclimation is mainly driven by increasing temperature (Welling et al. 2002, Kalberer et al. 2006) and occurs at a much faster rate than acclimation (Kalberer et al. 2007).

Current climate models predict an increase not only in the mean surface air temperature but also in the frequency and severity of erratic temperature events (IPCC 2014). Extended warm periods during autumn may, therefore, prevent timely frost acclimation, while the probability of early ('autumn') frost events remains high (Charrier et al. 2015). Furthermore, higher temperatures during mid-winter are likely to induce premature loss of FH (deacclimation), resulting in increasing plant vulnerability facing late ('spring') frost events (Kalberer et al. 2006, Pagter and Arora 2013). Late winter temperatures also promote within-bud ontogenetic development towards budburst, exposing tender organs, namely the flushing leaves and

blooming flowers, to late frost events (Saxe et al. 2001, Chamberlain et al. 2019). The transition periods in autumn and spring are the riskiest, as FH is relatively low and highly responsive to climate, while the probability of damageable freezing events is not negligible (Hanninen 2006, Charrier et al. 2018*a*).

Perennial tree species usually tolerate freezing events through two complementary mechanisms that can be tissue specific: (i) avoidance of intracellular ice formation by supercooling and (ii) tolerance to extracellular ice formation and to frost-induced desiccation (Levitt 1980). In many species, these mechanisms are often both present but in different tissues. In the extracellular compartment (apoplasm), solutes are expelled from the ice lattice towards a layer of up-concentrated unfrozen water (Hansen and Beck 1988). The difference in chemical potential between apoplasm and symplasm thus drives water efflux through plasma membrane in order to restore the osmotic balance, further concentrating symplasm, resulting in cell shrinkage (plasmolysis) and solute up-concentration (Arora 2018). Factors promoting extracellular ice formation as well as increased tolerance to desiccation are low molecular weight compounds (soluble sugars, organic acids, amino acids, lipids) and proteins (dehydrins; Sauter and van Cleve 1991, Sauter and Wellenkamp 1998, Hoch et al. 2002). These compounds protect cells, organelles, membranes and macromolecules by maintaining or replacing the solvation layer and maintaining their stability (Yoon et al. 1998, Kasuga et al. 2006, 2007). Solutes can also act as substrates for different metabolic pathways, when trees live on their own reserves.

Throughout the acclimation/deacclimation period, starch is hydrolyzed into soluble carbohydrates and resynthesized before budbreak (Sauter and van Cleve 1991, Sauter et al. 1998, Kaplan et al. 2006, Pagter et al. 2015, Charrier et al. 2018*b*). A concomitant decrease and re-increase in water content (WC) is also observed in various species (Salzman et al. 1996, Badulescu Valle 2003, Charrier et al. 2013*a*). Bulk water and solute contents are therefore crucial in predicting the change in FH at the branch and tissue level as observed in many species (Sakai 1960, Gusta et al. 2004, Morin et al. 2007, Charra-Vaskou et al. 2012, Charrier et al. 2013*a*).

Beyond the qualitative description of the relation between FH and these two factors (WC and solute content), both of them have been used as input variables to predict FH in various organs and tissues of *Juglans regia L.* cv Franquette (Poirier et al. 2010, Charrier et al. 2013*b*). Furthermore, temperature-induced carbohydrate synthesis allowed significant increase in FH even under cold deprivation treatment (Charrier and Améglio 2011). Despite the potential genericity of the involved mechanisms, this approach has not been extended to other species yet. One limitation lies in the chemical variability of soluble carbohydrates across species. Glucose, fructose and sucrose (GFS) have been selected in walnut as they represent over 90% of the total soluble carbohydrate content, but in other species, different molecules can be found, such as polyols in Rosaceae (Sakai 1966) or raffinose family oligosaccharides (RFOs) in some other tree species (Van Labeke and Volckaert 2010). Furthermore, different carbohydrate compounds showed contrasted effect with respect to FH (Sakai 1962).

As the contributions of WC and soluble carbohydrates and polyols (SCP) to FH have been demonstrated in many tree species as well as various organs and tissues, we hypothesize that this model can be further extended to a wide range of tree species. Moreover, as SCP composition differs across tree species, taking this composition into account could improve the robustness of the model. The aim of this study is, therefore, to demonstrate the interspecific genericity of the osmotic model through interaction between SCP and WC and to explore the relative contribution of each soluble carbohydrate in controlling FH in a wide range of tree species from different environments and sampling years. Four models were tested, differing in the way the SCP composition is taken into account, and calibrated both on each species separately and on the full dataset including all species. Models were compared using different statistical indexes and validated following two different approaches: a statistical validation on a random subset of the relevant dataset, and a cladistic approach using phylogenetically close species as the validation dataset.

Materials and methods

Plant material

The studied species were mainly angiosperm tree species, distributed among three orders from the rosids clade, supplemented with one conifer. One current year branch (longer than 40 cm) was sampled every 3 weeks per individual tree during two different periods: P_1 (October 2010–May 2011) and P_2 (August 2017–April 2018). During P_1, tree species were sampled in different locations: *Juglans regia* cv Franquette ($n = 5$ trees), *Juglans regia L.* × *nigra L.* ($n = 10$) and *Prunus persica L.* cv Redhaven ($n = 5$) in Crouel (45° 46.39′, 3° 8.67′, 338 m above sea level (a.s.l.)), *Fagus sylvatica L.* ($n = 5$) and *Prunus avium (L.) L.* ($n = 5$) in Fontfreyde (45° 42.23′, 2° 58.89′, 925 m a.s.l.), *Quercus petraea (Matt.) Liebl.* ($n = 5$) in Theix (45° 42.87′, E 3° 01.68′, 838 m a.s.l.), *Quercus robur L.* ($n = 5$) in Vic le Comte (45° 42.27′, E 2° 58.87′, 682 m a.s.l.) and *Larix decidua Mill.* in Lamartine (45° 42.95′, E 3° 01.74′, 829 m a.s.l., $n = 5$) and Orcival (45° 39.57′, 2° 49.44, 1148 m a.s.l., $n = 5$). During P_2, *J. regia* cv Franquette ($n = 3$), *J. regia* × *nigra* ($n = 6$) and *Malus domestica Borkh.*π cv Ariane ($n = 5$) were sampled in Crouel (Table 1). All trees were growing under natural conditions without irrigation nor fertilization.

Frost hardiness

Frost hardiness of living cells was assessed using the electrolyte leakage conductivity method on internodes (Zhang and Willison

Table 1. Species, location, periods and other information related to sampled species.

Species	Period	*n*	Age (years)	Site	Environment	Elevation (m a.s.l.)
Larix decidua	P_1	5	24	Lamartine	Mountain	829
		5	26	Orcival		1148
Quercus petraea	P_1	5	~40	Theix	Mountain	838
Quercus robur	P_1	5	~40	Vic le comte	Mountain	682
Fagus sylvatica	P_1	5	–	Fontfreyde	Mountain	925
Juglans regia cv Franquette	P_1	5	18	Crouel	Lowland	338
	P_2	3	26			
Juglans regia × *nigra*	P1	10	16	Crouel	Lowland	338
	P_2	6	24			
Prunus persica cv Redhaven	P_1	5	~15	Crouel	Lowland	338
Prunus avium	P_1	5	6	Fontfreyde	Mountain	925
Malus domestica	P_2	5	~15	Crouel	Lowland	338

1987, Sutinen et al. 1992). One current year branch per tree was cut into six 5-cm long pieces and exposed to different temperatures. Two samples were used as negative (unfrozen) and positive (fully damaged) controls at +5 and –80 °C, respectively. Four samples were exposed to four different sub-zero temperatures, depending on the expected FH range. During low FH period (i.e., May–September), −5, −10, −15 and −20 °C were typically used, whereas during high FH period (i.e., December–February), −10, −20, −30 and −40 °C were used. During frost acclimation (i.e., October and November) and deacclimation periods (i.e., March and April), samples were exposed to −7.5, −15, −22.5 and –30 °C. Samples were put in temperature-controlled boxes connected to a circulator bath (Ministat Huber, Offenburg, Germany). Temperature was controlled by an external Pt100 probe inserted in the chamber. Samples were exposed to one freeze–thaw cycle with temperature changes set at a steady rate of 5 K. h^{-1}. Once the target temperature was reached, it was held for an hour before thawing back to +5 °C. Air and sample surface temperatures were monitored every 20 s and averaged every 1 min using copper-constantan thermocouples and recorded by a data logger (CR1000, Campbell, Logan, CT, USA).

After temperature treatment, internodal sections were sliced into 1–2 mm thick slices and immersed into 15 ml of distilled–deionized water (Labwater, Veolia, Le Plessis-Robinson, France) in glass vials. The capped vials were placed on a horizontal gravity shaker plate (ST5, CAT, Staufen, Germany) for 24 h at +5 °C to limit bacterial growth and metabolic activity. The initial electric conductivity of the solution (C_1) was measured after warming the samples back to room temperature using an electric conduct meter (Portable conductivity meter ProfiLine Cond 3310, Bellingham + Stanley, Tunbridge Wells, UK). Vials were then autoclaved at 120 °C, 1 bar for 30 min and cooled down to room temperature before a second conductivity measurement was performed (C_2). Relative electrolytic leakage (REL) was computed as the ratio between C_1 and C_2 (Zhang and Willison 1987). The relation between REL and the minimum temperature reached by the sample (θ) was fit assuming a sigmoid relationship between both variables:

$$\mathrm{REL} = \frac{a}{1 + e^{b(c-\theta)}} + d \quad (1)$$

where θ is the temperature (in °C), b the slope at the inflection point c and a and ($a + d$) the lower and higher asymptotes of the relation, respectively.

Parameters were fitted by minimizing the sums of squares using non-linear regression analysis (ExcelStat software ver.2019.3.2). Frost hardiness was defined as the temperature at the inflection point c (i.e., corresponding to 50% induced damages; Repo and Lappi 1989).

Water content

Internodal sections of the samples were weighed using a microbalance (Sartorius, BP 210 S, accuracy = 0.1 mg) to obtain fresh matter (FM) and frozen in liquid nitrogen. Samples were then freeze-dried using a freeze dryer SMH 50, put in a proofer for 1 h and weighed again using the same microbalance to measure dry matter weight (DM). Water content was thus computed as:

$$\mathrm{WC} = \frac{\mathrm{FM} - \mathrm{DM}}{\mathrm{DM}} \quad (2)$$

with WC being the water content, FM and DM the fresh and dry weight, respectively.

Carbohydrate extraction and measurement

Freeze-dried samples (m > 1 g) were ground into a 0.12-mm grain size powder using a ball mill and 30 mg for each sample was used for carbohydrates extraction. The powder was mixed with 1 ml of mannitol solution (5 g. l^{-1}) in 80% ethanol in a micro vial and warmed at 80 °C in a water bath (Lauda Aqualine AL18, Lauda-Königshofen, Germany). Micro vials were shaken in a vortex mixer after 15 min of warming and centrifuged after 30 min (10 min, Hettich Mikro 220). The supernatant was purified by a vacuum filtration in a cartridge

containing 150 µl of AGX-1 anion-exchange resin, 100 µl of polyvinylpoly-pyrrolidone and 200 µl of activated charcoal. Two consecutive extractions were performed onto the solid using 1-ml ethanol–water (80–20 V/V), and an additional one with using 1-ml ethanol–water (50–50 V/V). The cartridge was finally rinsed using 1-ml ethanol–water (80–20 V/V). The liquid fraction was dried for SCs analysis (Thermo Scientific™ Savant™ SpeedVac™ DNA130 vacuum concentrator, Thermo Fisher Scientific Inc., Waltham, MA, USA) and the solid fraction for starch analysis.

Soluble carbohydrates and polyols (SCP) were diluted into 1 ml of distilled deionized water and measured using high-performance liquid chromatography with an amperometric detector (CLHP 817 Bioscan, Metrohm) coupled with a Metrosep column (Metrosep Carb2–250 × 4.0 mm, Metrohm Ltd, CH-9101 Herisau, Switzerland).

For starch measurement, the solid was mixed with 1 ml of NaOH (0.02 N) and autoclaved (1 h, 120 °C, 1 bar, AL02-01, Advantage-Lab). Starch samples were hydrolyzed with amyloglucosidase (EC 3.2.1.3, 150 U ml^{-1}) diluted in a citrate buffer (0.32 M, pH 4.2) and incubated in a water bath (1.5 h, 52 °C). In each well of a 96-well microplate, 12 µl of sample supernatant mixed with 180 µl of buffer (triethanolamine 0.75 M pH 7.6, NADP 0.015 M, ATP 0.040 M, $NaHCO_3$ 0.003 M) were added. Starch content was measured using a spectrophotometer (Power Wave 200, Biotek, Winooski, VT, USA) in a first time at wavelength 340 nm (initial measurement). A second measurement was performed after 40-min incubation under shaking with 10 µl of a solution containing 42 µl of hexokinase (EC 2.7.1.1, 30,000 U ml^{-1}), 100 µl of glucose-6-phosphate dehydrogenase (EC 1.1.1.49, 10,000 U/3 ml) and a buffer $(NH_4)_2SO_4$ (2.5 M, pH = 6).

Across species, the diversity in carbohydrate composition was assessed through the Shannon Index, an index usually used for measuring specific diversity in ecological studies:

$$H' = -\sum_{i=1}^{S} p_i \times \log_2(p_i) \quad (3)$$

where S is the total number of individual SCP detected in the study and p_i is the relative amount of carbohydrate or polyol i.

Correlations between physiological variables and FH

Four different functions were tested to model the relation between FH and the different variables either for all species combined into a bulk dataset (Table 2) or separately (see Table S1 available as Supplementary data at *Tree Physiology* Online). The first model, i.e., the JUG model, was originally calibrated on *J. regia* and considers the interaction of the sum of glucose, fructose and sucrose contents (GFS) with water content (WC) as:

$$FH = \alpha \times \frac{\ln(GFS)}{WC} + I \quad (4)$$

where FH is the frost hardiness in °C, GFS the sum of glucose, fructose and sucrose in mg. g DM^{-1} and WC the water content in g. g DM^{-1}, with parameters α (slope) and I (intercept).

The TOT model is similar to the JUG model but considers total soluble carbohydrates and polyols content (SCP), including glucose, fructose, sucrose, stachyose, raffinose, sorbitol, xylose, quebrachitol, myoinositol and an unidentified compound (N.I., in *L. decidua*) as the solute input variable:

$$FH = \alpha \times \frac{\ln(SCP)}{WC} + I \quad (5)$$

The OSMO model is similar to the TOT model, with the additional assumption that the cryoprotective effect of each solute (#i) is mediated by its partial osmotic potential π_i:

$$\pi_i = c_i \times R \times \theta \quad (6)$$

where R is the perfect gas constant (8.314 J. mol^{-1}. K^{-1}), θ the temperature set to 293.15 K for any compound (i ranging from 1 through 9, corresponding to glucose, fructose, sucrose, stachyose, raffinose, sorbitol, xylose, quebrachitol, myoinositol and an unidentified compound N.I., in *L. decidua*, respectively).

We further assumed that the compound volumic concentration (C_i, mol. m^{-3}) was proportional to its molar tissue content:

$$C_i \propto \frac{SCP_i}{MM_i} \quad (7)$$

where SCP_i is the mass tissue content of solute #i (g. g^{-1}) and MM_i the molar weight (g. mol^{-1}). Note that the molar weight of the non-identified SCP could not be computed and was assumed equal to the mean of the molar weights of other SCP.

The OSMO model was thus expressed as:

$$FH = \alpha \times \frac{\ln\left(\sum\left(\frac{SCP_i \times R \times \theta}{MM_i}\right)\right)}{WC} + I \quad (8)$$

The ISC model (for individual soluble carbohydrates) considers that the contribution of different carbohydrate molecules to FH is variable but not necessarily linked to π:

$$FH = \alpha \times \frac{\ln\left(\sum(p_i \times SCP_i)\right)}{WC} + I \quad (9)$$

where the p_i are free parameters additional to α and I.

Calibration and validation

The parameters α and I in the JUG, TOT and OSMO models were fitted by minimizing the sums of squares using a non-linear regression procedure (*nls* function in R ver.3.4.1; R Development

Table 2. Spearman's correlation coefficient (ρ) and *P*-value between frost hardiness (FH) and water content (WC), and the glucose, fructose and sucrose (GFS), soluble carbohydrates and polyols (SCP) and starch content (*P*-value, ***<0.001, **<0.01, *<0.05, ns > 0.05).

Species	Factor	ρ	*P*-value
J. regia	FH ~ WC	0.645	***
	FH ~ GFS	−0.790	***
	FH ~ SCP	−0.777	***
	FH ~ Starch	0.741	***
J. regia × *nigra*	FH ~ WC	0.630	***
	FH ~ GFS	−0.853	***
	FH ~ SCP	−0.845	***
	FH ~ Starch	0.782	***
F. sylvatica	FH ~ WC	0.100	ns
	FH ~ GFS	−0.812	***
	FH ~ SCP	−0.809	***
	FH ~ Starch	0.803	***
Q. petraea	FH ~ WC	0.091	ns
	FH ~ GFS	−0.763	***
	FH ~ SCP	−0.795	***
	FH ~ Starch	0.505	**
Q. robur	FH ~ WC	0.190	ns
	FH ~ GFS	−0.815	***
	FH ~ SCP	−0.885	***
	FH ~ Starch	0.480	***
M. domestica	FH ~ WC	0.294	*
	FH ~ GFS	−0.841	***
	FH ~ SCP	−0.564	***
	FH ~ Starch	0.663	***
P. avium	FH ~ WC	−0.275	ns
	FH ~ GFS	−0.837	***
	FH ~ SCP	−0.822	***
	FH ~ Starch	0.075	ns
P. persica	FH ~ WC	0.289	*
	FH ~ GFS	−0.765	***
	FH ~ SCP	−0.726	***
	FH ~ Starch	0.790	***
L. decidua	FH ~ WC	0.392	*
	FH ~ GFS	−0.461	**
	FH ~ SCP	−0.435	**
	FH ~ Starch	−0.100	ns
All species	FH ~ WC	0.431	***
	FH ~ GFS	−0.610	***
	FH ~ SCP	−0.772	***
	FH ~ Starch	0.540	***

Core Team 2019). The ISC model had $k = 7$ to 11 individual parameters, reflecting the number of individual carbohydrates included in the relevant dataset. Considering that the cryoprotective effect, if any, should be positive, the k parameters p_i corresponding to each carbohydrate detected were assigned a lower bound of 0.0001 (under which threshold it would be considered non-effective) and estimated with the *port* algorithm of the *nls* non-linear least square fitting function in *R*. If the *port* algorithm could not converge when all k solutes were included as input variables, the $(k - 1)$ restricted models including only $(k - 1)$ solutes were tested for convergence, leading to a stepwise procedure discarding non-effective variables. Thus, each SCP could be considered in three ways in the ISC model: non-detected (ND) in the dataset, detected but non-effective ($p_i < 0.0001$) and effective.

The models were compared using different indexes such as root mean squared error (RMSE), adjusted *R*-squared (Adj.R^2), and corrected Akaike index criterion (AICc, Akaike 1974, Hurvich and Tsai 1995), computed as:

$$\mathrm{RMSE} = \sqrt{\frac{\sum_{i=1}^{n} \left(\hat{y}_i - y_i\right)^2}{n}} \tag{10}$$

$$\mathrm{Adj.}R^2 = 1 - \frac{n \bullet (n-1) \bullet \mathrm{RMSE}^2}{(n-k) \bullet \sum_{i=1}^{n} (y_i - \overline{y})^2} \tag{11}$$

$$\mathrm{AICc} = 2\,n\left[\log(\mathrm{RMSE}) + \frac{k}{n-k-1}\right] \quad (12)$$

with $\hat{y}_i$ the values simulated by the model for an individual i, y_i the observed values for an individual i, k the number of parameters, n the number of observations and $\bar{y}$ their mean.

When two models are evaluated on the same dataset, the better is the one that has lower RMSE and AICc and/or higher Adj.R^2. Bias was assessed comparing the slope of the regression of the predicted values against the observed values (pred. vs obs.) and the $y = x$ line (see Figure 4).

Two different approaches were used to validate the models, namely the statistical and the cladistic validations. The statistical validation was performed (i) at the species level, (ii) at the botanical family level, merging all species belonging to a given family (Fagaceae, Juglandaceae and Rosaceae) and (iii) at the full angiosperm species dataset level. For each dataset, the models were calibrated on one randomly selected half of the dataset (calibration dataset) and tested on the other half of the dataset (validation dataset). This operation was independently performed 1000 times and tested the quantitative homogeneity of the variables. The cladistic validation checked the validity of the models for each species independently, testing the homogeneity of the parameters according to the clades on which the models were calibrated. The cladistic validation was performed on datasets merging the species (i) by genus (*Juglans*, *Prunus* and *Quercus*), (ii) by family (Juglandaceae, Fagaceae and Rosaceae) and (iii) all of the angiosperms. For each dataset, the models were validated according to the one clade (species, genus or family) left out cross-validation, i.e., calibration was performed on all but one clade and validation on that remaining clade.

The RMSE was computed as the mean distance between observed and simulated values on the calibration dataset. Prediction RMSE (RMSEP) was computed through observed vs simulated values obtained on an external (validation) dataset. The model validation was discussed in relation to the difference between RMSE and RMSEP.

Statistical analysis

The normality of each variable distribution was tested using the Shapiro–Wilk test with alpha = 0.05. The homogeneity in variance was tested for each variable using the Fisher test with alpha = 0.05. Differences in means were compared using Student's *t* test or Welch test when variances were not equal. The tests of correlations between variables were performed using Spearman's test. All statistical analysis were performed using R software ver.3.4.1 (R Development Core Team 2019).

Results

Seasonal changes in FH and physiological variables

All species exhibited a similar pattern, regardless of the period and location, including frost acclimation in autumn and deacclimation in late winter and spring (Figure 1). However, frost acclimation rate was highly variable across species: from -0.26 ± 0.01 to -0.17 ± 0.01 °C. day^{-1}, for *J. regia* × *nigra* (P_1) and *J. regia* (P_2), respectively. Maximum FH was also highly different across species: from -39.3 ± 0.5 for *J. regia* × *nigra* (P_1) through -26.6 ± 0.5 °C for *J. regia* (P_2).

Seasonal changes in water, soluble carbohydrates, polyols and starch contents exhibited similar patterns across species, locations and periods (Figures 1 and 2): high hydration state during the summer, dehydration during autumn (mostly during September) and spring rehydration (from March in *L. decidua*, until April in *Q. petraea*, *Q. robur*, *F. sylvatica* and *J. regia*). In August and September, starch content for *J. regia* (P_2), *J. regia* × *nigra* (P_2) and *M. domestica* strongly increased while the SCP contents remained constant (Figure 2). From October until December, starch content decreased for all species while SCP concomitantly increased. The SCP and starch contents remained relatively constant during December and January. The maximum SCP contents (Table 3) observed in winter were normally distributed ($W = 0.91$, $P = 0.23$), ranging from 60.7 ± 1.9 (*P. avium*) to 94.3 ± 4.7 mg. g^{-1} DM (*L. decidua*). In February, starch content increased while SCP decreased in all species.

The SCP composition (Table 3) was highly contrasted across species. A low diversity was observed in the Juglandaceae family ($H' \leq 1.3$; Table 3), with GFS representing more than 90% of the SCP. Higher diversity was observed in the Fagaceae family ($1.38 \leq H' \leq 1.73$), although GFS also represented more than 90% of SCP. In this family, sucrose was the main carbohydrate but was highly variable across species (ca 70, 55 and 40%, for *F. sylvatica*, *Q. robur* and *Q. petraea*, respectively; see Figure S1 available as Supplementary data at *Tree Physiology* Online). In the Rosaceae family, the diversity in SCP was lower in *M. domestica* ($H' = 1.39$) than in *Prunus* species ($H' \geq 2.00$), in relation to the high amount of sorbitol (ca 70, 35 and 50%, for *M. domestica*, *P. avium* and *P. persica*, respectively). High diversity in SCP ($H' = 2.12$) was observed in *L. decidua* (see Figure S2 available as Supplementary data at *Tree Physiology* Online). Seasonal peaks in the relative distribution of SCP were mainly observed for glucose (*F. sylvatica*, *J. regia*, *J. regia* × *nigra*, *L. decidua*, *Q. petrae*, *Q. robur* and *P. persica*) and fructose (*J. regia* and *J. regia* × *nigra*). For further tests, *L. decidua* (two locations), *J. regia* (P_1 and P_2) and *J. regia* × *nigra* (P_1 and P_2) were pooled at the species scale, as they did not exhibit significant differences.

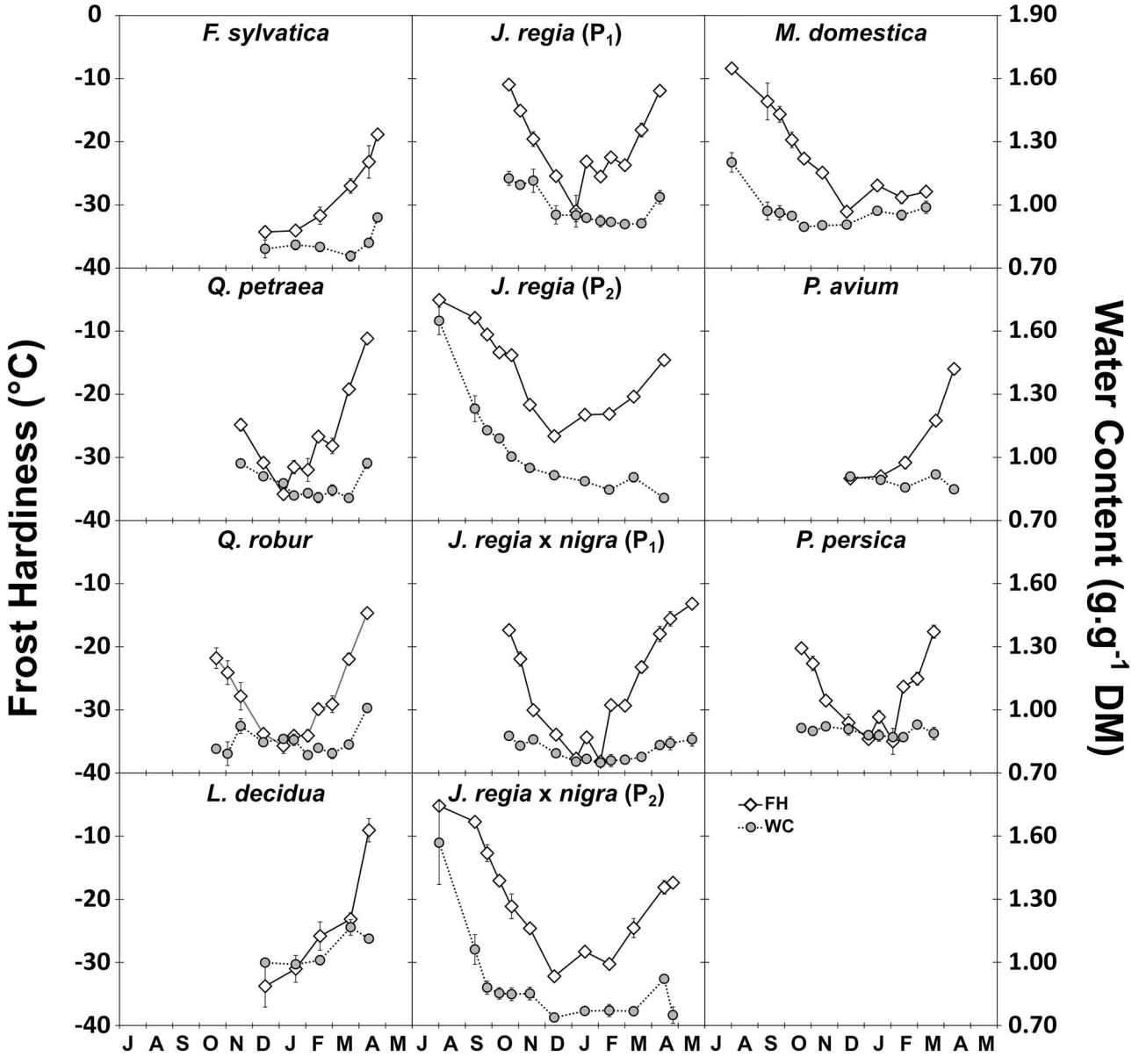

Figure 1. Seasonal changes in frost hardiness and water content for *F. sylvatica* ($n = 5$), *J. regia* P_1 ($n = 5$), *J. regia* P2 ($n = 3$), *J. regia* × *nigra* P_1 ($n = 10$), *J. regia* × *nigra* P_2 ($n = 6$), *L. decidua* ($n = 10$), *M. domestica* ($n = 5$), *P. avium* ($n = 5$), *P. persica* ($n = 5$), *Q. petraea* ($n = 5$) and *Q. robur* ($n = 5$). Symbols and bars represent means ± standard errors per sampling date in *n* replicates.

Frost hardiness depending on physiological variables

On the whole dataset, FH was positively correlated to WC (Table 2; $\rho = 0.43$; $P < 0.001$), although, at the species level, the correlation was not significant for some species such as *F. sylvatica*, *P. avium*, *Q. petraea* and *Q. robur* ($P = 0.71$; 0.18; 0.56; 0.17) and relatively weak for *L. decidua*, *M. domestica* and *P. persica* ($P = 0.01$; 0.04; 0.04). Frost hardiness was negatively correlated with GFS ($\rho = -0.61$; $P < 0.001$) and even more with SCP ($\rho = -0.77$; $P < 0.001$). Correlations between FH and GFS or SCP were similar in all species (means of Spearman's $\rho = -0.77 \pm 0.04$ and -0.74 ± 0.05, $P = 0.37$; for GFS and SCP, respectively), with the notable exception of *M. domestica* ($\rho = -0.56$ and -0.84 for GFS and SCP, respectively). Spearman's ρ coefficients between FH and SCP or GFS were significant but lower in *L. decidua* than in all other species (Spearman's $\rho = -0.45$ for both GFS and SCP). Considering all species, correlation of FH with starch was weaker than with GFS and SCP content but stronger than with WC (Table 2; $\rho = 0.540$; $P < 0.001$). At the species level, the correlation coefficients of FH with starch content were very close to or lower than with GFS or SCP but higher than with WC. The significance of WC with respect to FH was highlighted by the comparison between *M. domestica*, *J. regia* and *J. regia* × *nigra*. *Malus domestica* was more frost tolerant in August compared with *Juglans* sp. with lower WC and similar SCP in the three species (Figure 2). During winter, although *J.*

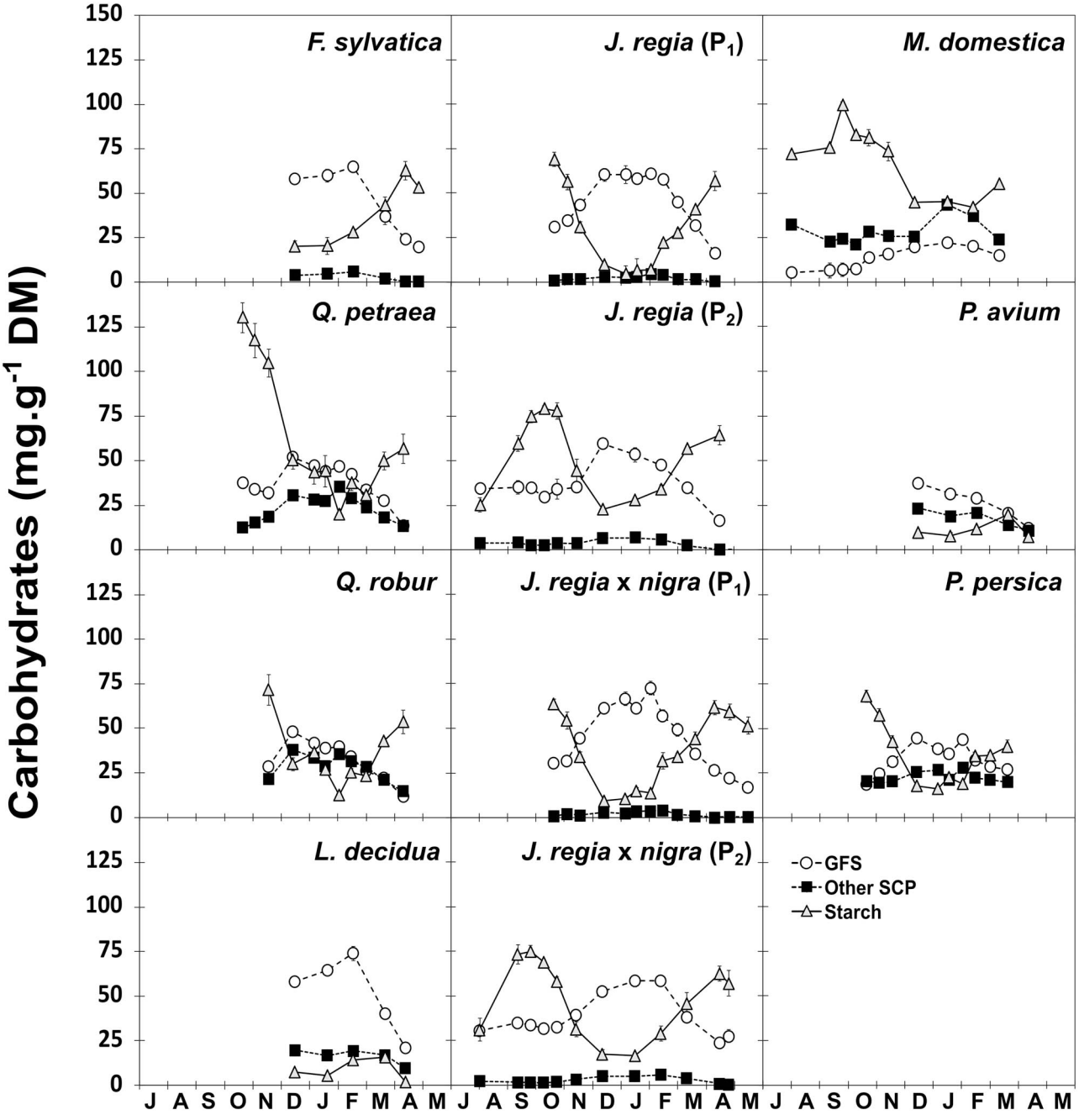

Figure 2. Seasonal changes in soluble carbohydrate and polyols content for *F. sylvatica* ($n = 5$), *J. regia* P_1 ($n = 5$), *J. regia* P_2 ($n = 3$), *J. regia* × *nigra* P_1 ($n = 10$), *J. regia* × *nigra* P_2 ($n = 6$), *L. decidua* ($n = 10$), *M. domestica* ($n = 5$), *P. avium* ($n = 5$), *P. persica* ($n = 5$), *Q. petraea* ($n = 5$) and *Q. robur* ($n = 5$). GFS represents the sum of glucose, fructose and sucrose; 'other SCP' represents the remaining measured soluble carbohydrates and polyols. Symbols and bars represent the means ± standard errors per sampling date in *n* replicates.

regia and *J. regia* × *nigra* exhibited similar levels of GFS for all sampling dates, *J. regia* × *nigra* had lower WC and FH.

Modeling FH depending on the interaction between carbohydrates and WC

Four different models were calibrated on the whole dataset and at the species level through four different computations of carbohydrates and polyols (Figure 3). The JUG model, using GFS as the solute input variable, exhibited a good efficiency in most species (Table 4) with RMSE lower than 3 °C for *P. avium* (2.65 °C) and *F. sylvatica* (2.67 °C), and lower than 4 °C in *J. regia* (3.42 °C), *M. domestica* (3.62 °C) and *P. persica* (3.93 °C). The accuracy remained limited but still reasonable in the other species: *J. regia* × *nigra* (4.37 °C), *Q. petraea* (4.54 °C) and *Q. robur* (5.29 °C). However, in *L. decidua*, GFS model failed to predict FH correctly (RMSE = 8.18 °C).

Table 3. Different indicative values with respect to ecophysiological winter parameters: frost hardiness (frost acclimation rate, FAR; frost deacclimation rate, FDR; maximum of frost hardiness, FH_{Max}), water content (minimum of water content, WC_{Min}) and soluble carbohydrates and polyols (maximum of glucose, fructose and sucrose, GFS_{Max}; maximum of soluble carbohydrates and polyols, SCP_{Max}; GFS on SCP, GFS/SCP; Shannon index of SCP, H'). Numbers are means ± standard error (SE) in *n* replicates. Minimum values are in italic and maximum values are in bold.

Species	FAR (°C. day^{-1})	FDR (°C. day^{-1})	FH_{Max} (°C)	WC_{Min} (g. g DM^{-1})	GFS_{Max} (mg. g DM^{-1})	SCP_{Max} (mg. g DM^{-1})	GFS/SCP	H'
F. sylvatica	NA	0.14 ± 0.01	−34.5 ± 0.7	0.80 ± 0.01	65.03 ± 1.53	70.64 ± 0.85	94.8 ± 0.8	1.38
Q. petraea	−0.22 ± 0.03	**0.22 ± 0.02**	−36.5 ± 0.9	0.85 ± 0.01	49.03 ± 1.72	85.83 ± 2.27	94.4 ± 0.4	1.73
Q. robur	−0.19 ± 0.01	0.21 ± 0.01	−36.7 ± 0.7	0.83 ± 0.02	53.27 ± 3.17	86.67 ± 2.51	93.3 ± 0.5	1.65
J. regia	−0.20 ± 0.01	0.14 ± 0.02	*−27.7 ± 0.5*	0.92 ± 0.02	64.83 ± 1.77	69.42 ± 1.55	94.2 ± 0.3	1.27
J. regia (P_1)	−0.22 ± 0.01	0.16 ± 0.02	−28.5 ± 0.5	0.94 ± 0.02	67.25 ± 2.64	70.44 ± 2.78	96.1 ± 0.3	1.30
J. regia (P_2)	*−0.17 ± 0.01*	*0.10 ± 0.01*	−26.6 ± 0.5	0.88 ± 0.01	60.78 ± 0.42	67.70 ± 0.29	91.2 ± 0.5	1.28
J. regia × *nigra*	−0.26 ± 0.01	0.19 ± 0.01	−36.8 ± 0.9	*0.76 ± 0.01*	69.86 ± 2.78	74.50 ± 2.77	95.4 ± 0.2	1.11
J. regia × *nigra* (P_1)	**−0.26 ± 0.01**	**0.22 ± 0.01**	**−39.3 ± 0.5**	*0.76 ± 0.01*	**74.99 ± 3.27**	78.63 ± 3.57	**96.3 ± 0.3**	1.11
J. regia × *nigra* (P_2)	−0.25 ± 0.02	0.14 ± 0.01	−32.7 ± 0.6	*0.76 ± 0.00*	61.29 ± 2.54	67.62 ± 2.78	93.6 ± 0.4	*1.09*
M. domestica	−0.18 ± 0.01	NA	−31.3 ± 0.4	0.94 ± 0.01	*23.25 ± 1.59*	65.85 ± 4.29	*30.5 ± 1.4*	1.39
P. avium	NA	0.20 ± 0.01	−33.8 ± 0.4	0.89 ± 0.00	37.35 ± 0.86	*60.75 ± 1.88*	59.4 ± 1.6	**2.19**
P. persica	−0.19 ± 0.02	**0.22 ± 0.01**	−35.1 ± 0.9	0.88 ± 0.02	46.42 ± 2.10	75.41 ± 3.29	58.4 ± 0.8	2.00
L. decidua	NA	0.20 ± 0.03	−35.2 ± 1.3	**1.00 ± 0.01**	73.79 ± 3.76	**94.33 ± 4.75**	75.0 ± 0.8	2.12

The TOT model predicted lower errors than the JUG model in *F. sylvatica* and *Q. robur* (RMSE = 2.66 and 5.10 °C, respectively). In *J. regia*, *J. regia* × *nigra* and *L. decidua*, accuracy remained similar to the JUG model. In *P. avium*, *P. persica*, *M. domestica* and *Q. petraea*, the model was less accurate than the JUG model. Finally, the TOT model was efficient for *F. sylvatica*, *J. regia* and *J. regia* × *nigra*, but not for the Rosaceae family and the *Quercus* genus. Surprisingly, the JUG model was more efficient than the TOT model in the Rosaceae species although these species contained a high proportion of sorbitol (30–86%). Seasonal changes in sorbitol content were indeed relatively low in this clade (Figure 2).

The OSMO model exhibited higher RMSE and AICc and lower Adj.R^2 than the JUG and TOT models for all species. The ISC model was the most accurate in all species providing relatively good predictions in all angiosperm species (between 1.82 and 3.83 °C for *P. avium* and *J. regia* × *nigra*, respectively). Despite a higher number of parameters (8 vs 2), the ISC model had also lower AICc than the other models for all angiosperm species. As suggested by the mono-factorial correlations in *L. decidua* (Table 2), the models did not predict FH properly in this species (mean RMSE = 8.08 vs 3.92 °C in *L. decidua* and all other species, respectively) and lower Adj.R^2 (Adj.R^2 = 0.298 vs 0.644 in *L. decidua* and all species, respectively; Table 2). This species has thus been discarded for the next steps of calibration and validation at different levels, restricting the dataset to angiosperm species.

The JUG model calibrated on the full angiosperm dataset presented lower Adj.R^2 and higher RMSE (5.98 °C) and AICc than the other models (Table 5; Figure 4A). The TOT (Figure 4B) and OSMO (Figure 4C) models exhibited similar accuracy (4.81 and 5.03 °C for SCP and OSMO, respectively), Adj.R^2 and AICc. The ISC model exhibited lower RMSE (4.07 °C) and AICc and higher Adj.R^2 (Figure 4D). According to these results, glucose, sucrose, raffinose and sorbitol are significantly correlated to FH, whereas fructose, stachyose, myoinositol and quebrachitol can be considered as less or ineffective. Among the significantly effective carbohydrates, glucose and raffinose exhibited higher parameter values (1.26 ± 0.40 and 1.00 ± 0.40, respectively) than sucrose and sorbitol (0.22 ± 0.04 and 0.39 ± 0.10, respectively), meaning that, for the same concentration, FH is enhanced. Surprisingly, the non-identified carbohydrate, although present sporadically and in very small proportions in *P. avium* and *P. persica* (0.73 < % < 2.57), was considered effective for FH (7.15 ± 3.60, $P = 0.06$).

Model validation

The different models were statistically validated in almost all species with RMSEP < 1.5 × RMSE (Table 6), except the ones with very low degree of freedom for the ISC model such as *F. sylvatica* (1.49 ± 0.01 and 3.48 ± 0.05 °C for RMSE and RMSEP, respectively) and *P. avium* (1.64 ± 0.01 and 2.78 ± 0.03 °C for RMSE and RMSEP, respectively). The RMSE on the calibration dataset was approximately 3.0 °C for ISC, 4.4 °C for JUG and TOT and 4.9 °C for OSMO. On the validation dataset, the accuracy was lower but remained in the same range for all species and clades: RMSEP ca 3.7 °C for ISC, 4.7 °C for JUG 4.8 °C for TOT and 5.3 °C for OSMO. Across models, the rank between models was conserved in all species and clades for both RMSE and RMSEP (ISC < JUG < TOT < OSMO), meaning that ISC was the most accurate and OSMO the least accurate.

For further insight into the genericity of the models, the predictive ability of models calibrated on subset of species

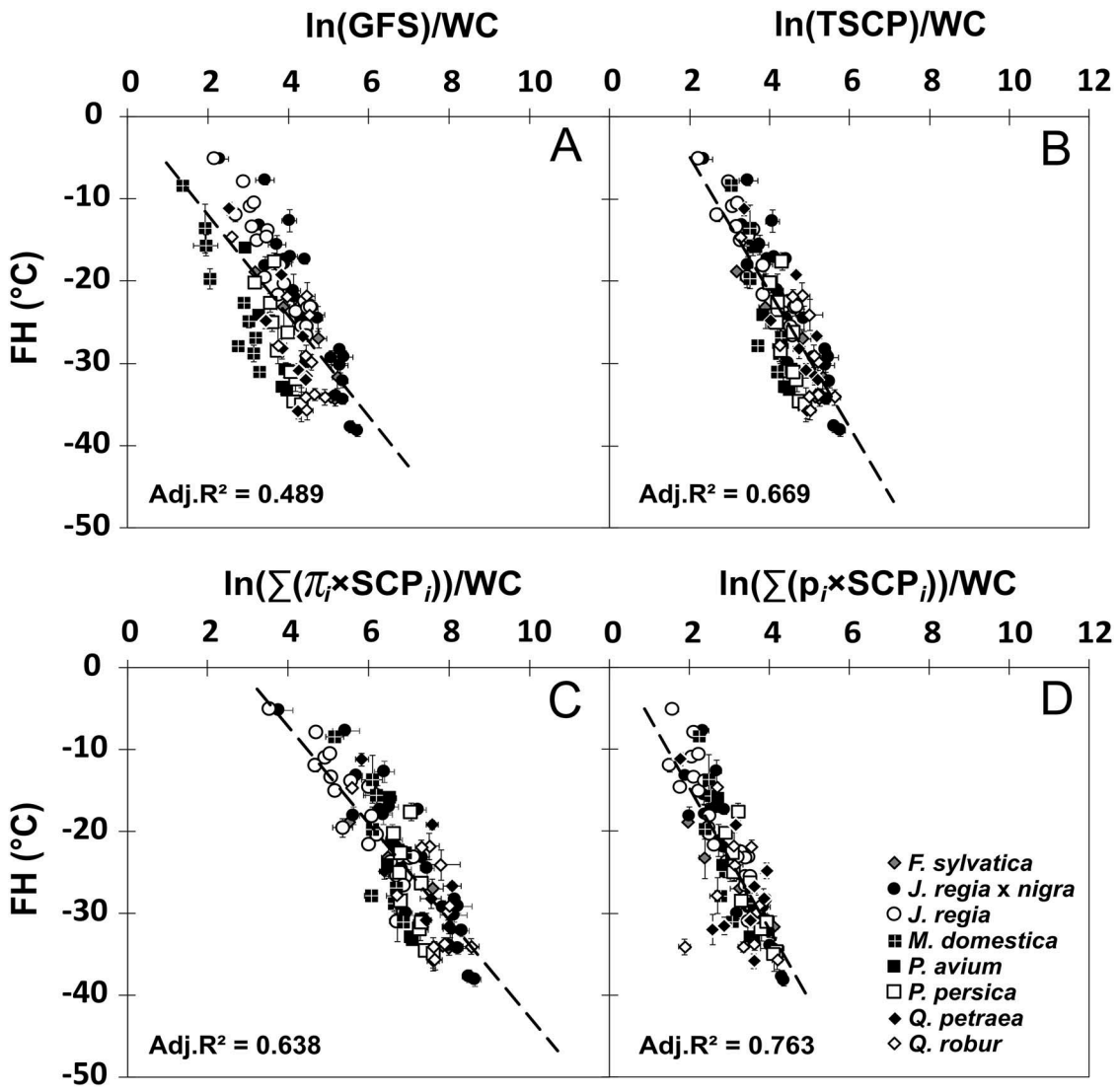

Figure 3. Frost hardiness (FH) depending on the interaction between water content and different expressions of soluble carbohydrates and polyols according to sum of GFS (A), the sum of SCP (B) or the sum of SCP, each soluble carbohydrate *i* being weighted by its osmotic potential π_i (C) or by a parameter p_i fitted by the ISC model (D) calibrated on angiosperms data.

was measured on an independent species from the same clade. For the *Juglans* and *Quercus* genus, the ISC model exhibited lower RMSE and RMSEP than the other models (Table 7). The models calibrated on *J. regia* × *nigra* were more accurate on *J. regia*, but the reverse was not true. In the Fagaceae family, RMSEP was lower than RMSE when JUG, TOT and OSMO models were not calibrated on *F. sylvatica*, due to the limited number of observations for this species. Conversely, for the ISC model, removing this species in the calibration dataset gave higher RMSEP than RMSE (3.11 and 7.49 °C, for RMSE and RMSEP, respectively). In the Rosaceae family, contrasted results were obtained depending on the composition of the calibration dataset. When *P. avium* was included in the calibration dataset, the JUG and ISC models failed to predict accurate values, whereas the reverse was not necessarily observed.

For all angiosperms, each species, except *M. domestica*, allowed accurate FH prediction. The ISC model exhibited lower RMSE and RMSEP (4.06 ± 0.02 and 4.42 ± 0.19 °C for RMSE and RMSEP, respectively) than the JUG (5.92 ± 0.06 and 6.46 ± 0.72 °C for RMSE and RMSEP, respectively), the TOT (4.06 ± 0.04 and 5.01 ± 0.38 °C for RMSE and RMSEP, respectively) and the OSMO model (5.03 ± 0.04 and 5.18 ± 0.37 °C for RMSE and RMSEP, respectively).

Discussion

Despite inter-specific and inter-annual variabilities in winter ecophysiological parameters, this study highlighted the link between tissue composition and FH of living cells over various tree species, among three orders from the rosids clade. The relationship between WC and SCP was shared across

Table 4. Calibration of four frost hardiness models (JUG, TOT, OSMO and ISC) at different cladistics scale (species, family, angiosperm): degree of freedom (Df), root mean squared error (RMSE), adjusted R^2 (Adj.R^2) and corrected Akaike information criterion (AICc). All models for all species were highly significant ($P < 0.001$). For each species, the best model is in bold characters.

Species	Model	Df	RMSE	Adj.R^2	AICc
J. regia	JUG	88	3.42	0.755	482.7
	TOT	88	3.49	0.744	486.5
	OSMO	88	3.58	0.731	491.1
	ISC	**82**	**3.03**	**0.793**	**474.5**
J. regia × *nigra*	JUG	192	4.37	0.766	1129.1
	TOT	192	4.38	0.766	1129.5
	OSMO	192	4.65	0.736	1152.8
	ISC	**186**	**3.83**	**0.815**	**1089.9**
Juglandaceae	JUG	282	4.14	0.781	1623.2
	TOT	282	4.16	0.780	1621.2
	OSMO	282	4.42	0.751	1660.3
	ISC	**276**	**3.67**	**0.829**	**1562.3**
F. sylvatica	JUG	14	2.67	0.714	83.8
	TOT	14	2.66	0.716	83.7
	OSMO	14	3.05	0.629	88.0
	ISC	**8**	**1.93**	**0.824**	**87.4**
Q. petraea	JUG	42	4.54	0.570	264.3
	TOT	42	5.11	0.455	274.7
	OSMO	42	5.83	0.289	286.4
	ISC	**36**	**3.16**	**0.756**	**248.3**
Q. robur	JUG	53	5.29	0.376	345.5
	TOT	53	5.10	0.418	341.6
	OSMO	53	5.54	0.315	350.6
	ISC	**47**	**2.63**	**0.825**	**283.8**
Fagaceae	JUG	113	4.89	0.470	701.7
	TOT	113	4.91	0.467	698.4
	OSMO	113	5.44	0.346	725.8
	ISC	**107**	**3.33**	**0.741**	**622.3**
M. domestica	JUG	48	3.62	0.754	276.8
	TOT	48	4.96	0.539	308.2
	OSMO	48	5.62	0.407	320.7
	ISC	**42**	**3.23**	**0.796**	**280.6**
P. avium	JUG	23	2.65	0.832	126.2
	TOT	23	4.04	0.609	147.4
	OSMO	23	5.07	0.386	158.6
	ISC	**16**	**1.90**	**0.874**	**135.0**
P. persica	JUG	48	3.93	0.564	285.0
	TOT	48	4.16	0.512	290.7
	OSMO	48	4.83	0.342	305.7
	ISC	**41**	**2.91**	**0.719**	**273.4**
Rosaceae	JUG	123	4.51	0.610	741.3
	TOT	123	4.66	0.584	745.7
	OSMO	123	5.28	0.466	781.0
	ISC	**116**	**3.92**	**0.688**	**716.4**
L. decidua	JUG	39	8.18	0.276	295.0
	TOT	39	8.21	0.271	295.3
	OSMO	39	8.47	0.224	297.8
	ISC	**33**	**7.45**	**0.287**	**303.5**

this whole range of species, but not with a conifer species. Thanks to the specific composition in carbohydrate molecules, this study also highlighted that the differential effect of independent carbohydrate molecules was not only linked to their 'bulk' osmotic potential as computed from their average tissue content.

Frost hardiness vs physiological variables

Frost hardiness in the studied species presented classical dynamics in over-wintering branches (Morin et al. 2007, Charrier et al. 2011, Mayoral et al. 2015). Acclimation and deacclimation were observed in *Juglans sp.*, *Quercus sp*, *M.*

Table 5. Comparison between the four different models of FH depending on grouped or individualized soluble carbohydrate and polyols: JUG (1), TOT (2), OSMO (3) and ISC model (4) calibrated on all data. SCP_i, MM_i, p_i and WC represent the sugar and polyol content, the osmotic potential and the parameter adjusted of the carbohydrate *i*, respectively. *R* and θ are parameters representing the perfect gas constant (8.314 J. Mol^{-1}. K^{-1}) and the temperature (293.15 K), respectively. The degree of freedom (Df), the root mean squared error (RMSE), adjusted R^2 (Adj.R^2), corrected Akaike information criterion (AICc), slope (α) and intercept (I) with their respective estimate, standard errors (SE) and degree of significance (*P*-value, ***<0.001, **<0.01, *<0.05, ns >0.05). ND means that the sugar was not detected in the tree. Parameters adjusted for individual soluble carbohydrates i are presented for fructose (fr), glucose (gl), myoinositol (mi), quebrachitol (qu), raffinose (ra), sorbitol (so), sucrose (su), stachyose (st) and non-identified (n.i.).

Model	Df	RMSE	Adj.R^2	AICc	Parameter (Estimate ±SE)
(1) $FH = \alpha \times \frac{\ln(GFS)}{WC} + I$	522	5.98	0.486	3367	**$\alpha = -6.13 \pm 0.27$***** $I = 0.28 \pm 1.13$ ns
(2) $FH = \alpha \times \frac{\ln(SCP)}{WC} + I$	522	4.81	0.668	3140	**$\alpha = -8.24 \pm 0.25$***** **$I = 11.74 \pm 1.13$*****
(3) $FH = \alpha \times \frac{\ln\left(\sum\left(\frac{SCP_i \times R \times \theta}{MM_i}\right)\right)}{WC} + I$	522	5.03	0.636	3187	**$\alpha = -5.92 \pm 0.20$***** **$I = 16.49 \pm 1.37$*****
(4) $FH = \alpha \times \frac{\ln\left(\sum\left(P_i \times SCP_i\right)\right)}{WC} + I$	516	4.07	0.758	2982	**$\alpha = -9.63 \pm 0.54$***** **$I = 5.92 \pm 1.76$***** $fr = 0.15 \pm 0.10$ ns **$gl = 1.27 \pm 0.42$**** mi < 0.0001 qu < 0.0001 **$ra = 1.01 \pm 0.41$*** **$so = 0.39 \pm 0.10$***** st < 0.0001 **$su = 0.22 \pm 0.04$***** $n.i. = 7.15 \pm 3.75$ ns

Significant parameters, relative estimates and standard errors are indicated in bold.

domestica and *P. persica* and only deacclimation in *F. sylvatica*, *L. decidua* and *P. avium*. The seasonal changes in FH could be correlated to the changes in WC through a relatively weak but significant correlation, explaining ca 26% of the variance in FH (Table 3), as observed in different organs of *J. regia* (Charrier et al. 2013*b*). Stronger correlations have been observed in more homogeneous plant material like branch from the same species (Poirier et al. 2010, Saadati et al. 2019). Starch and SCP contents exhibited similar dynamics across species and periods, with hydrolysis during acclimation and resynthesis during deacclimation. Significant and negative correlations between FH and GFS or SCP were observed in all species (Table 2). The composition in SCP was contrasted among species and clades, qualitatively and quantitatively (H' range from 1.11 to 2.19). Correlations between FH and GFS was observed in *P. persica* (Shin et al. 2015) and *J. regia* (Charrier et al. 2013*b*), while other compounds such as raffinose family oligosaccharides were mentioned in *Rubus idaeus* (Palonen and Junttila 2002) or *Hydrangea sp.* (Pagter et al. 2008). In *L. decidua*, despite significant correlation between FH and GFS or SCPs, the four models exhibited very low accuracy and efficiency. Although the changes in WC and SCP were similar to other angiosperm species, it may suggest that other components could affect FH (e.g., polyphenols or amino acids; Bilkova et al. 1999, Zwiazek et al. 2001). The genericity of the tested models thus remained limited to angiosperm trees.

Model structure and calibration

Considering the time lapse between changes in WC to SCP, WC is more strongly correlated to FH during the early stage of acclimation and late stage of deacclimation, whereas SCP during the late stage of acclimation and early stage of deacclimation. This temporal gap is translated into the non-linear formalism of the models, through reverse and logarithm transformation for WC and GFS/SCP, respectively.

Depending on the scale, the different formalisms exhibited contrasting accuracies. The JUG model was relatively efficient at the species and family level (RMSEP < 5 °C), except for *Quercus* species. This model uses, as input variable, the main carbohydrates from *J. regia* to predict FH across organs and tissues (Améglio et al. 2004, Charrier et al. 2013*b*). Using the total amount of carbohydrates and polyols as an input variable did not improve the accuracy at the species scale, although GFS to SCP varied from less than 60% in the Rosaceae to more than 90% of the SCP in Juglandaceae and Fagaceae. Glucose, sucrose and fructose indeed co-varied with FH in all species.

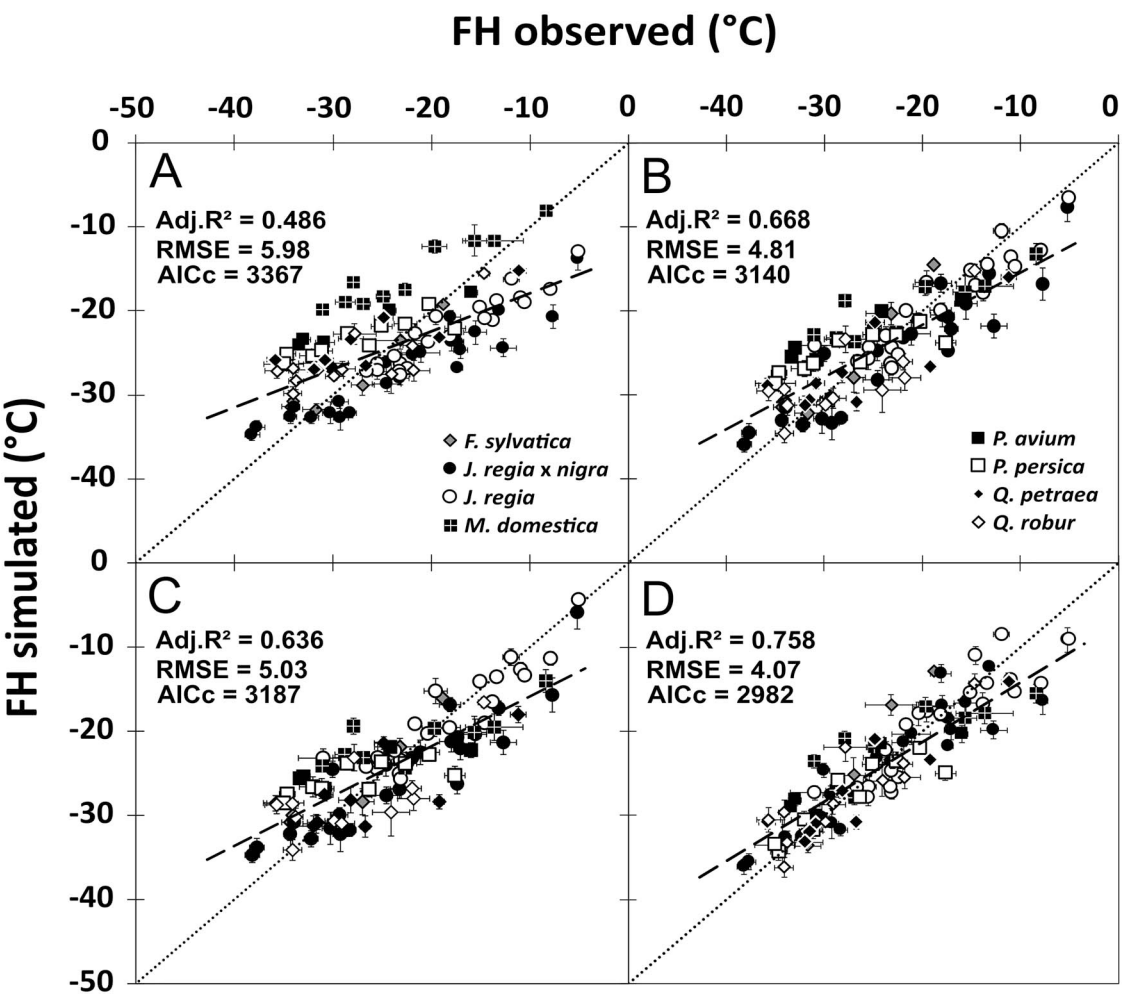

Figure 4. Correlations between frost hardiness observed (FH observed) and frost hardiness simulated (FH simulated) by the JUG model (A), the TOT model (B), the OSMO model (C) and the ISC model (D) calibrated on angiosperm data. Symbols and bars represent means ± standard errors per sampling date and species: *F. sylvatica* ($n = 5$), *J. regia* ($n = 5$ for P_1 and $n = 3$ for P_2), *J. regia* × *nigra* ($n = 10$ for P_1 and $n = 6$ for P_2), *L. decidua* ($n = 10$), *M. domestica* ($n = 5$), *P. avium* ($n = 5$), *P. persica* ($n = 5$), *Q. petraea* ($n = 5$) and *Q. robur* ($n = 5$).

At the broadest scale (i.e., angiosperms), the TOT model was the most robust and accurate (ca 4.8 °C). However, in the Rosaceae family, the lower accuracy and efficiency of the TOT model with respect to JUG implies that sorbitol (ca 35% of SCPs) would not contribute to change in FH. Different compounds would differently contribute to FH as previously shown by infiltration of different compounds at the same concentration (Sakai 1962). Such a differential effect of carbohydrate and polyol molecules onto FH was further tested via other formalisms (i.e., OSMO and ISC models).

The OSMO model assumed that each solute would exhibit homogeneous concentration across tissues and cells and trigger a proportional effect to its osmotic potential in decreasing the freezing point (−1.86 °C. mol^{-1}. l; Hansen and Beck 1988, Chang 1991, Cavender-Bares 2005). Although the OSMO model performed better than the JUG and not much worse than the TOT model at the angiosperm scale, the systematic lower accuracies and efficiencies at the species or clade scale did not support the assumption of osmotic control of bulk branch FH. Furthermore, the highest accuracies and efficiencies provided by the ISC model at each tested scale suggest differential contribution of individual molecules, although carbohydrates have suggested to act non-specifically (Klotke et al. 2004). Several other roles have been highlighted to protect cells from frost damage. Solutes stabilize membranes and macromolecules, replacing water molecules within a solvation layer under extended frost-induced desiccation (Yoon et al. 1998, Pearce 1999, Arora 2018). Carbohydrates can also be used as a substrate supplying various metabolic pathways for the synthesis of other cryoprotectants or to respond to frost damages.

To consider these various roles, each compound was assumed to independently correlate with FH (ISC model). The contribution of each compound may vary depending on the acclimation or deacclimation period but the procedure used, combining statistical and biological validation, provided robust results at different scales. At the species scale,

Table 6. Statistical validation of the four models at the angiosperms (all species), family (Fagaceae, Juglandaceae and Rosaceae) and species scales. For each species, parameters were fitted on the half of the data randomly selected and RMSE was computed. Parameters were applied on the other half of the data and RMSEP was computed. Means of RMSE and RMSEP ± standard error (SE) were computed on 1000 replicates. Angiosperms groups all species; Fagaceae groups *F. sylvatica*, *Q. petraea* and *Q. robur*; Juglandaceae groups *J. regia* and *J. regia* × *nigra*; and Rosaceae groups *M. domestica, P. avium* and *P. persica*. Parameters is the number of parameters and Df the residual degree of freedom for the model of calibration. Data in bold represent when RMSEP is 50% higher than RMSE.

Clade	Model	Parameters	Df	RMSE ± SE	RMSEP ± SE
F. sylvatica	JUG	2	6	4.02 ± 0.02	4.53 ± 0.02
	TOT	2	6	4.14 ± 0.02	4.67 ± 0.02
	OSMO	2	6	4.61 ± 0.03	5.28 ± 0.03
	ISC	**7**	**1**	**1.49 ± 0.01**	**3.48 ± 0.05**
Q. petraea	JUG	2	20	4.79 ± 0.01	5.21 ± 0.01
	TOT	2	20	4.98 ± 0.01	5.41 ± 0.01
	OSMO	2	20	5.51 ± 0.01	6.11 ± 0.01
	ISC	7	15	2.94 ± 0.01	3.82 ± 0.02
Q. robur	JUG	2	26	5.15 ± 0.02	5.59 ± 0.02
	TOT	2	26	5.01 ± 0.01	5.32 ± 0.01
	OSMO	2	26	5.41 ± 0.01	5.86 ± 0.02
	ISC	7	21	2.49 ± 0.01	3.14 ± 0.01
Fagaceae	JUG	2	56	4.85 ± 0.01	5.01 ± 0.01
	TOT	2	56	4.85 ± 0.01	5.04 ± 0.01
	OSMO	2	56	5.38 ± 0.01	5.58 ± 0.01
	ISC	8	50	3.20 ± 0.01	3.67 ± 0.01
J. regia	JUG	2	43	3.71 ± 0.01	4.07 ± 0.01
	TOT	2	43	4.00 ± 0.01	4.40 ± 0.01
	OSMO	2	43	4.46 ± 0.01	4.96 ± 0.02
	ISC	7	38	2.93 ± 0.02	3.26 ± 0.02
J. regia × *nigra*	JUG	2	95	3.78 ± 0.02	4.19 ± 0.02
	TOT	2	95	4.12 ± 0.02	4.57 ± 0.01
	OSMO	2	95	4.65 ± 0.02	5.23 ± 0.02
	ISC	7	90	3.75 ± 0.01	4.02 ± 0.01
Juglandaceae	JUG	2	140	4.48 ± 0.01	4.60 ± 0.01
	TOT	2	140	4.53 ± 0.01	4.67 ± 0.01
	OSMO	2	140	5.01 ± 0.01	5.14 ± 0.01
	ISC	7	135	3.62 ± 0.01	3.79 ± 0.01
M. domestica	JUG	2	23	3.70 ± 0.01	4.05 ± 0.01
	TOT	2	23	4.12 ± 0.01	4.49 ± 0.01
	OSMO	2	23	4.62 ± 0.01	5.09 ± 0.01
	ISC	8	17	3.06 ± 0.01	3.67 ± 0.01
P. avium	JUG	2	11	3.65 ± 0.02	4.13 ± 0.02
	TOT	2	11	4.06 ± 0.02	4.61 ± 0.02
	OSMO	2	11	4.66 ± 0.02	5.35 ± 0.02
	ISC	**7**	**6**	**1.64 ± 0.01**	**2.78 ± 0.03**
P. persica	JUG	2	23	3.73 ± 0.01	4.08 ± 0.01
	TOT	2	23	4.01 ± 0.01	4.39 ± 0.01
	OSMO	2	23	4.49 ± 0.01	4.98 ± 0.01
	ISC	7	18	2.81 ± 0.01	3.96 ± 0.01
Rosaceae	JUG	2	61	4.66 ± 0.01	4.81 ± 0.01
	TOT	2	61	4.73 ± 0.01	4.90 ± 0.01
	OSMO	2	61	5.31 ± 0.01	5.48 ± 0.01
	ISC	9	54	3.83 ± 0.01	4.28 ± 0.01
Angiosperms	JUG	2	260	5.96 ± 0.00	6.02 ± 0.01
	TOT	2	260	4.80 ± 0.00	4.84 ± 0.00
	OSMO	2	260	5.02 ± 0.00	5.07 ± 0.00
	ISC	9	253	4.03 ± 0.00	4.17 ± 0.00

Table 7. Cladistic validation of the different models at the angiosperms (all species), family (Fagaceae and Rosaceae) and genera (*Juglans*, *Prunus* and *Quercus*) scales. Parameters were fitted on the data calibration and RMSE was computed. Parameters were applied on the data validation and RMSEP was computed. Data in bold represent when RMSEP is 50% higher than RMSE (*i.e.*, not validated).

Clade	Data calibration	Data validation	JUG		TOT		OSMO		ISC	
			RMSE	RMSEP	RMSE	RMSEP	RMSE	RMSEP	RMSE	RMSEP
Juglans	*J. regia* × *nigra*	*J. regia*	4.37	3.74	4.38	3.76	4.65	4.17	3.83	3.56
	J. regia	*J. regia* × *nigra*	3.42	4.55	3.49	4.51	3.58	4.93	3.03	4.17
Quercus	*Q. petraea*	*Q. petraea*	5.29	4.98	5.11	5.24	5.54	5.88	2.63	3.79
	Q. robur	*Q. robur*	4.54	6.00	5.10	5.21	5.83	5.59	3.16	3.80
Fagaceae	*Q. petraea* + *Q. robur*	*F. sylvatica*	5.10	3.53	5.13	3.25	5.68	3.62	**3.11**	**7.49**
	Q. robur + *F. sylvatica*	*Q. petraea*	4.86	5.05	4.72	5.24	5.14	5.92	3.24	3.83
	Q. petraea + *F. sylvatica*	*Q. robur*	4.46	5.36	4.68	5.19	5.33	5.57	3.18	3.78
Prunus	*P. persica*	*P. avium*	3.93	4.23	4.16	5.40	4.83	5.51	**2.91**	**9.24**
	P. avium	***P. persica***	**2.65**	**5.47**	4.04	5.48	5.07	5.53	**1.90**	**5.86**
Rosaceae	*P. avium* + *P. persica*	***M. domestica***	**3.89**	**10.11**	4.42	5.10	5.03	5.74	**3.12**	**9.82**
	M. domestica + *P. persica*	*P. avium*	4.58	4.28	4.68	4.72	5.25	5.46	3.84	4.91
	M. domestica + *P. avium*	***P. persica***	**4.02**	**6.02**	4.71	4.96	5.50	5.04	**2.96**	**7.16**
Angiosperms	All but species of validation	*J. regia*	6.04	6.16	5.04	3.57	5.28	3.63	4.11	4.27
		J. regia × *nigra*	5.78	7.03	4.80	5.10	5.09	5.09	4.12	4.06
		F. sylvatica	6.05	2.83	4.85	3.42	5.07	3.57	4.07	4.23
		Q. petraea	6.00	5.90	4.78	5.11	4.95	5.89	4.06	4.44
		Q. robur	6.01	5.79	4.76	5.25	4.95	5.71	4.02	4.56
		M. domestica	**5.60**	**10.18**	4.71	5.73	4.95	5.82	3.91	5.52
		P. avium	5.91	7.43	4.71	6.64	4.96	6.39	4.05	4.61
		P. persica	5.96	6.37	4.77	5.24	5.00	5.35	4.12	3.70

sucrose, glucose and fructose were considered efficient (i.e., exhibiting a significantly non-null parameter estimate) in all species. Raffinose and stachyose were considered efficient in Juglandaceae (both) and Fagaceae (raffinose only) families. Myoinositol, quebrachitol and sorbitol were not considered efficient, except sorbitol in *P. avium*. At the angiosperm scale, all SCPs were considered efficient but myoinositol, quebrachitol and stachyose. Sucrose and raffinose have been reported to enhance FH in many species, including herbaceous and woody species (Taulavuori et al. 1997, Palonen et al. 2000, Cox and Stushnoff 2001, Gusta et al. 2004). Sucrose and raffinose were the only two compounds significantly correlated to change in FH in both xylem and bark tissues in *Hydrangea* (Pagter et al. 2011). This would explain why they are the most relevant compounds in our study, performed on bulk branches, whereas other compounds can exhibit different dynamics across tissues.

The ISC model was the more informative, exhibiting the highest accuracy and efficiency, but, due to higher number of parameters, was more complex to calibrate. The parameter convergence towards lowest RMSE required a close analysis of the SCP composition depending on the dataset (Winde et al. 2017). Lower limits for each parameter were set to 10^{-4} forcing the algorithm to converge. In some cases, the parameter estimates were equal to this bound, suggesting that the mathematically optimal value could have been null or even negative. Negative parameter values have been observed using unbound calibration procedure (data not shown). Mechanistically, this would suggest that some compounds could decrease FH. However, this could only been verified if we would have access to the whole metabolome without spatial discrimination at the tissue and cell scales.

The approach used here was limited to carbohydrate and polyol compounds. However, other osmotically active molecules have been previously identified in FH or desiccation tolerance studies, such as such as proline (Withers and King 1979), other amino acids (Smith 1968), fructo- and gluco-oligosaccharides (Hincha et al. 2002). The spatial distribution of solutes across tissues or within the cell may also affect their activity. At the cellular scale, vacuole is a major compartment, representing up to 90–95% of the cell volume. Various compounds can cross the tonoplast, e.g., by passive diffusion down a concentration gradient or through active transport for sucrose (Pollock and Kingston-Smith 1997, Neuhaus 2007). Carbohydrates accumulate in the vacuole during cold acclimation treatment in *Arabidopsis thaliana* (Nägele and Heyer 2013). However, there is no clear picture if it could result in over-accumulation of carbohydrate in the cytosol compared with vacuole (Nägele and Heyer 2013, Weiszmann et al. 2018). Another uncertainty may arise from the water content measurement as this method is very sensitive to the delay between sampling and weighing in relation to specific density of the sample. The WC data did not exhibit large spatio-temporal variability, although the calibration of the different models did support the significance of this factor.

Existing models have been developed for non-stressed plants, through empirical relations between FH and environmental drivers (temperature and photoperiod, e.g., Timmis et al. 1994, Leinonen 1996, Ferguson et al. 2011, Charrier et al. 2018*a*). To our knowledge, the only model that takes physiological measurements into account uses pH of the cell effusate as an input variable (Taulavuori et al. 1997). However, how this pH would be affected by environmental conditions is not clear. On the contrary, the interconversion between starch and GFS has been successfully modeled in walnut and an extension to other species would be feasible (Charrier et al. 2018*b*). Based on physiological measurement, this model can explicitly take into account the cumulative effect of stress factor, entailing water and carbon status and therefore frost acclimation (Charrier et al. 2020).

Conclusion and perspectives

This study highlighted the interaction between water content and soluble carbohydrates and polyols contents for frost hardiness prediction in various angiosperm species. The ISC model explicitly assessed the individual impact of compounds on frost hardiness. Sucrose and raffinose appeared as the best predictors of changes in frost hardiness, whereas polyols did not appear to be efficient. Finally, the TOT model was the most effective for large-scale studies aiming to compare FH across species, while the ISC model was the most efficient at the family or species scales. The respective contribution of each compound provides a clue as to which metabolic pathways to target to improve frost resistance in different angiosperm species.

Supplementary data

Supplementary data for this article are available at *Tree Physiology* Online.

Acknowledgments

This work was supported both by INRAE-department of AgroEnv 50%, and by Region Auvergne Rhône-Alpes 50% in the context of a PhD grant to R.B. The authors acknowledge Christophe Serre and Brigitte Saint-Joanis for their respective help in frost hardiness measurements and physiological data measurements.

Funding

This work was supported by INRAE- Agroecosystem department (50%), and Region Auvergne Rhône-Alpes (50%) in the context of a PhD grant to R.B.

Conflict of interest

None declared.

References

Akaike H (1974) A new look at statistical-model identification. IEEE Trans Automat Contr A 19:716–723.

Améglio T, Decourteix M, Alves G, Valentin V, Sakr S, Julien JL, Petel G, Guilliot A, Lacointe A (2004) Temperature effects on xylem sap osmolarity in walnut trees: evidence for a vitalistic model of winter embolism repair. Tree Physiol 24:785–793.

Arora R (2018) Mechanism of freeze-thaw injury and recovery: a cool retrospective and warming up to new ideas. Plant Sci 270:301–313.

Arora R, Rowland LJ (2011) Physiological research on winter-hardiness: deacclimation resistance, Reacclimation ability, Photoprotection strategies, and a cold acclimation protocol design. HortScience 46:1070–1078.

Badulescu Valle RV (2003) Mechanisms of frost adaptation and freeze damage in grapevine buds. PhD thesis, University of Hohenheim, Germany, p 45.

Bilkova J, Albrechtova J, Opatrna J (1999) Histochemical detection and image analysis of non-specific esterase activity and the amount of polyphenols during annual bud development in Norway spruce. J Exp Bot 50:1129–1138.

Cavender-Bares J (2005) Impacts of freezing on long-distance transport in woody plants. In: Holbrook NM, Zwieniecki M (eds) Vascular transport in plants. New Phytologist. Elsevier Inc., Oxford, pp 401–424.

Chamberlain CJ, Cook BI, García de Cortázar-Atauri I, Wolkovitch EM (2019) Rethinking false spring risk. Glob Chang Biol 25:2209–2220.

Chang R (1991) Chemistry. McGraw-Hill Education, New York, NY.

Charra-Vaskou K, Charrier G, Wortemann R, Beikircher B, Cochard H, Ameglio T, Mayr S (2012) Drought and frost resistance of trees: a comparison of four species at different sites and altitudes. Ann For Sci 69:325–333.

Charrier G, Améglio T (2011) The timing of leaf fall affects cold acclimation by interactions with air temperature through water and carbohydrate contents. Environ Exp Bot 72:351–357.

Charrier G, Bonhomme M, Lacointe A, Ameglio T (2011) Are budburst dates, dormancy and cold acclimation in walnut trees (*Juglans regia* L.) under mainly genotypic or environmental control? Int J Biometeorol 55:763–774.

Charrier G, Cochard H, Ameglio T (2013*a*) Evaluation of the impact of frost resistances on potential altitudinal limit of trees. Tree Physiol 33:891–902.

Charrier G, Poirier M, Bonhomme M, Lacointe A, Ameglio T (2013*b*) Frost hardiness in walnut trees (*Juglans regia* L.): how to link physiology and modelling? Tree Physiol 33:1229–1241.

Charrier G, Ngao J, Saudreau M, Ameglio T (2015) Effects of environmental factors and management practices on microclimate, winter physiology, and frost resistance in trees. Front Plant Sci 6:259.

Charrier G, Chuine I, Bonhomme M, Ameglio T (2018*a*) Assessing frost damages using dynamic models in walnut trees: exposure rather than vulnerability controls frost risks. Plant Cell Environ 41:1008–1021.

Charrier G, Lacointe A, Ameglio T (2018*b*) Dynamic modeling of carbon metabolism during the dormant period accurately predicts the changes in frost hardiness in walnut trees *Juglans regia* L. Front Plant Sci 9:1746.

Charrier G, Martin-Stpaul N, Damesin C, Delpierre N, Hänninen H, Torres-Ruiz J, Davi H (2020) Interaction of drought and frost in tree ecophysiology: rethinking the timing of risks. Annals of Forest Science (in press). Recommended by Peer Community in Forest and Wood Science, https://hal.archives-ouvertes.fr/hal-02475505v4.

Christersson L (1978) Influence of photoperiod and temperature on development of frost hardiness in seedlings of *Pinus sylvestris* and *Picea abies*. Physiol Plant 44:288–294.

Cox SE, Stushnoff C (2001) Temperature-related shifts in soluble carbohydrate content during dormancy and cold acclimation in *Populus tremuloides*. Can J For Res 31:730–737.

Ferguson JC, Tarara JM, Mills LJ, Grove GG, Keller M (2011) Dynamic thermal time model of cold hardiness for dormant grapevine buds. Ann Bot 107:389–396.

Gusta LV, Wisniewski M, Nesbitt NT, Gusta ML (2004) The effect of water, sugars, and proteins on the pattern of ice nucleation and propagation in acclimated and nonacclimated canola leaves. Plant Physiol 135:1642–1653.

Hanninen H (2006) Climate warming and the risk of frost damage to boreal forest trees: identification of critical ecophysiological traits. Tree Physiol 26:889–898.

Hansen J, Beck E (1988) Evidence for ideal and non-ideal equilibrium freezing of leaf water in frosthardy ivy (*Hedera helix*) and winter barley (*Hordeum vulgare*). Bot Acta 101:76–82.

Hincha DK, Zuther E, Hellwege EM, Heyer AG (2002) Specific effects of fructo-and gluco-oligosaccharides in the preservation of liposomes during drying. Glycobiology 12:103–110.

Hoch G, Popp M, Körner C (2002) Altitudinal increase of mobile carbon pools in *Pinus cembra* suggests sink limitation of growth at the Swiss treeline. Oikos 98:361–374.

Hurvich CM, Tsai CL (1995) Model selection for extended quasi-likelihood models in small samples. Biometrics 51:1077–1084.

IPCC (2014) Climate change 2014: synthesis report. IPCC, Geneva.

Kalberer SR, Wisniewski M, Arora R (2006) Deacclimation and reacclimation of cold-hardy plants: current understanding and emerging concepts. Plant Sci 171:3–16.

Kasuga J, Mizuno K, Miyaji N, Arakawa K, Fujikawa S (2006) Role of intracellular contents to facilitate supercooling capability in beech (*Fagus crenata*) xylem parenchyma cells. CryoLetters 27:305–310.

Kalberer SR, Leyva-Estrada N, Krebs SL, Arora R (2007) Frost dehardening and rehardening of floral buds of deciduous azaleas are influenced by genotypic biogeography. Environ Exp Bot 59:264–275.

Kaplan F, Sung DY, Guy CL (2006) Roles of beta-amylase and starch breakdown during temperatures stress. Physiol Plant 126:120–128.

Kasuga J, Mizuno K, Arakawa K, Fujikawa S (2007) Anti-ice nucleation activity in xylem extracts from trees that contain deep supercooling xylem parenchyma cells. Cryobiology 55:305–314.

Klotke J, Kopka J, Gatzke N, Heyer AG (2004) Impact of soluble sugar concentrations on the acquisition of freezing tolerance in accessions of *Arabidopsis thaliana* with contrasting cold adaptation–evidence for a role of raffinose in cold acclimation. Plant Cell Environ 27:1395–1404.

Leinonen I (1996) A simulation model for the annual frost hardiness and freeze damage of Scots pine. Ann Bot 78:687–693.

Levitt J (1980) Plant plasma-membrane water permeability and slow freezing-injury-reply. Plant Cell Environ 3:159–160.

Mayoral C, Strimbeck R, Sanchez-Gonzalez M, Calama R, Pardos M (2015) Dynamics of frost tolerance during regeneration in a mixed (pine-oak-juniper) Mediterranean forest. Trees Struct Funct 29:1893–1906.

Morin X, Ameglio T, Ahas R, Kurz-Besson C, Lanta V, Lebourgeois F, Miglietta F, Chuine I (2007) Variation in cold hardiness and carbohydrate concentration from dormancy induction to bud burst among provenances of three European oak species. Tree Physiol 27: 817–825.

Nägele T, Heyer AG (2013) Approximating subcellular organisation of carbohydrate metabolism during cold acclimation in different natural accessions of *Arabidopsis thaliana*. New Phytol 198:777–787.

Neuhaus HE (2007) Transport of primary metabolites across the plant vacuolar membrane. FEBS Lett 581:2223–2226.

Pagter M, Arora R (2013) Winter survival and deacclimation of perennials under warming climate: physiological perspectives. Physiol Plant 147:75–87.

Pagter M, Jensen CR, Petersen KK, Liu FL, Arora R (2008) Changes in carbohydrates, ABA and bark proteins during seasonal cold acclimation and deacclimation in *Hydrangea* species differing in cold hardiness. Physiol Plant 134:473–485.

Pagter M, Lefevre I, Arora R, Hausman JF (2011) Quantitative and qualitative changes in carbohydrates associated with spring deacclimation in contrasting *Hydrangea* species. Environ Exp Bot 72: 358–367.

Pagter M, Andersen UB, Andersen L (2015) Winter warming delays dormancy release, advances budburst, alters carbohydrate metabolism and reduces yield in a temperate shrub. AoB Plants 7:plv024.

Palonen P, Junttila O (2002) Carbohydrates and winter hardiness in red raspberry. In: Brennan RM, Gordon SL, Williamson B (eds) Proceedings of the Eighth International Rubus and Ribes Symposium, Vol. 1 and 2. International Society Horticultural Science, Leuven, pp 573–577.

Palonen P, Buszard D, Donnelly D (2000) Changes in carbohydrates and freezing tolerance during cold acclimation of red raspberry cultivars grown in vitro and in vivo. Physiol Plant 110:393–401.

Pearce RS (1999) Molecular analysis of acclimation to cold. Plant growth regulation 29:47–76.

Poirier M, Lacointe A, Ameglio T (2010) A semi-physiological model of cold hardening and dehardening in walnut stem. Tree Physiol 30:1555–1569.

Pollock CJ, Kingston-Smith AH (1997) The vacuole and carbohydrate metabolism. In: Advances in botanical research, Vol. 25. Academic Press, pp 195–215.

R Development Core Team (2019) R: a language and environment for statistical computing. R Foundation for Statistical Computing, Vienna, Austria. https://www.r-project.org/.

Repo T, Lappi J (1989) Estimation of standard error of impedance-estimated frost resistance. Scand J For Res 4:67–74.

Saadati S, Baninasab B, Mobli M, Gholami M (2019) Measurements of freezing tolerance and their relationship with some biochemical and physiological parameters in seven olive cultivars. Acta Physiol Plant 41:1–11.

Sakai A (1960) Relation of sugar content to frost-hardiness in plants. Nature 185:698–699.

Sakai A (1962) Studies on the frost-hardiness of woody plants; 1.The causal relation between sugar content and frost-hardiness. Contrib from Inst Low Temp Sci B11:1–40.

Sakai A (1966) Studies of frost hardiness in woody plants. 2. Effect of temperature on hardening. Plant Physiol 41:353.

Salzman RA, Bressan RA, Hasegawa PM, Ashworth EN, Bordelon BP (1996) Programmed accumulation of LEA-like proteins during desiccation and cold acclimation of overwintering grape buds. Plant Cell Environ 19:713–720.

Smith D (1968) Varietal chemical differences associated with freezing resistance in forage plants. Cryobiology 5:148–159.

Sauter JJ, van Cleve B (1991) Biochemical and ultrastructural results during starch-sugar-conversion in ray parenchyma cells of *Populus* during cold adaptation. J Plant Physiol 139:19–26.

Sauter JJ, Wellenkamp S (1998) Seasonal changes in content of starch, protein and sugars in the twig wood of *Salix caprea* L. Holzforschung Int J Biol Chem Phys Technol Wood 52: 255–262.

Sauter JJ, Elle D, Witt W (1998) A starch granule bound endoamylase and its possible role during cold acclimation of parenchyma cells in poplar wood (*Populus* × *canadensis* Moench *robusta*). J Plant Physiol 153:739–744.

Saxe H, Cannell MGR, Johnsen B, Ryan MG, Vourlitis G (2001) Tree and forest functioning in response to global warming. New Phytol 149:369–399.

Shin H, Kim K, Oh Y, Yun SK, Oh SI, Sung J, Kim D (2015) Carbohydrate changes in peach shoot tissues and their relationship to cold acclimation and deacclimation. Hortic J 84:21–29.

Sutinen ML, Palta JP, Reich PB (1992) Seasonal differences in freezing stress resistance of needles of *Pinus nigra* and *Pinus resinosa*—evaluation of the electrolyte leakage method. Tree Physiol 11:241–254.

Taulavuori K, Niinimaa A, Laine K, Taulavuori E, Lähdesmäki P (1997) Modelling frost resistance of scots pine seedlings using temperature, daylength and pH of cell effusate. Plant Eco 133: 181–189.

Timmis R, Flewelling J, Talbert C (1994) Frost injury prediction model for Douglas-fir seedlings in the Pacific Northwest. Tree Physiol 14:855–869.

Van Labeke MC, Volckaert E (2010) Evaluation of electrolyte leakage for detecting cold acclimatization in six deciduous tree species. In: Sramek F, Dostalkova J, Chaloupakova S (eds) I International Symposium on Woody Ornamentals of the Temperate Zone, Vol. 1. International Society for Horticultural Science, Leuven, pp 403–410.

Weiszmann J, Fürtauer L, Weckwerth W, Nägele T (2018) Vacuolar sucrose cleavage prevents limitation of cytosolic carbohydrate metabolism and stabilizes photosynthesis under abiotic stress. FEBS J 285:4082–4098.

Welling A, Moritz T, Palva ET, Junttila O (2002) Independent activation of cold acclimation by low temperature and short photoperiod in hybrid aspen. Plant Physiol 129:1633–1641.

Winde J, Andersen UB, Kjaer KH, Pagter M (2017) Variation in freezing tolerance, water content and carbohydrate metabolism of floral buds during deacclimation of contrasting blackcurrant cultivars. Acta Physiol Plant 39:1–14.

Withers LA, King PJ (1979) Proline: a novel cryoprotectant for the freeze preservation of cultured cells of *Zea mays* L. Plant Physiol 64:675–678.

Yoon YH, Pope JM, Wolfe J (1998) The effects of solutes on the freezing properties of and hydration forces in lipid lamellar phases. Biophys J 74:1949–1965.

Zhang MIN, Willison JHM (1987) An improved conductivity method for the measurement of frost hardiness. Can J Bot 65: 710–715.

Zwiazek JJ, Renault S, Croser C, Hansen J, Beck E (2001) Biochemical and biophysical changes in relation to cold hardiness. In: Colombo S, Bigras F (eds) Conifer cold hardiness. Kluwer Academic Publishers, Dordrecht, pp 165–186.